

Energy-Straggling Measurements of Heavy Charged Particles in Thick Absorbers

C. TSCHALÄR*

Rutherford High Energy Laboratory, Chilton, Berkshire, England

AND

H. D. MACCABEE†

M.R.C. Radiobiology Unit, Biophysics Group, Harwell, Didcot, Berkshire, England

(Received 22 May 1969; revised manuscript received 22 August 1969)

Energy-straggling distributions of 20- and 49-MeV protons and 80-MeV helium ions have been measured for energy losses of 10 to 92% of the initial kinetic energy. Aluminum and gold absorbers were used, and the residual energy spectra were measured with lithium-drifted silicon semiconductor detectors. Experimental results show very good agreement with the theories of Payne and Tschalär, provided that broadening due to atomic binding is taken into account, and disagreement with the Bohr theory for energy losses greater than 20%. In particular, as the particle beam slows down in the absorber, the variance of the energy distribution increases faster than the absorber thickness traversed, and a degree of skewness (i.e., a low-energy "tail") is introduced at very large energy losses.

I. INTRODUCTION

THE energy loss of fast heavy charged particles in matter is caused mainly by discrete, random collisions with atomic electrons. The statistical nature of the ionization and excitation processes results in fluctuations of energy losses of an initially monoenergetic particle beam as it passes through an absorber. Consequently, the energy spectrum of the beam is gradually widened as the particles penetrate the absorber. The resulting distribution of kinetic energies T after a pathlength x in the absorber will be denoted by $f(T, x)$.

In this study we consider the problem of "thick" absorbers, that is, cases in which energy losses are *not* small compared to the initial energy T_0 . More specifically, we deal with cases where the change in the single-collision spectrum due to slowing down of the beam may not be neglected in calculations of the energy-loss distribution. The problem of thin absorbers has been dealt with previously.¹

The purpose of this study was to measure accurately the energy distribution of protons and helium ions in thick homogeneous absorbers, and to test the relevant theories.

II. THEORY

Several authors have treated the problem of calculating $f(T, x)$ for thick absorbers.²⁻⁶ In cases where particle

losses due to complete stopping are insignificant, it has been shown⁴ that the distributions $f(T, x)$ may be well described by their mean energy T_{av} , their variance σ_2 , and their reduced third central moment γ_3 , where

$$T_{av}(x) \equiv \int_0^{\infty} f(T, x) T dT,$$

$$\sigma_n(x) \equiv \int_0^{\infty} f(T, x) (T - T_{av})^n dT,$$

and

$$\gamma_m(x) \equiv \sigma_m(\sigma_2)^{-m/2} \text{ for integers } n \text{ and } m.$$

The standard deviation $\sigma \equiv \sigma_2^{1/2}$ is a measure of the width of $f(T, x)$, and γ_3 indicates its skewness ($\gamma_3 = 0$ for symmetric distributions).

A considerable number of calculations of $f(T, x)$ are based on a simplified, nonrelativistic, free-electron form of the single-collision energy-loss probability per unit thickness. This quantity $P(Q, T)$ was described, e.g., by Lewis⁷ and has the form

$$P(Q, T) = \begin{cases} \frac{1}{2}(k/T)Q^{-2}, & \text{for } Q_{\min} \leq Q \leq Q_{\max} \\ 0, & \text{otherwise} \end{cases} \quad (1)$$

$$Q_{\max} = 4\mu(1+\mu)^{-2}T \equiv \epsilon T,$$

$$Q_{\min} = I^2/(\epsilon T),$$

where Q is the energy loss in the collision, $k = 2\pi e^4 z^2 ZN/\mu$, e is the electron charge, z is the particle charge number, Z is the atomic number of the absorber, N is the number of absorber atoms per unit volume, μ is the ratio of electron mass to particle mass, and I is the mean excitation potential of the absorber.

The lower limit Q_{\min} affects only the stopping power κ_1 appreciably, where

$$\kappa_1 = \int_0^{\infty} P(Q, T) Q dQ. \quad (2)$$

* Present address: Schweizerisches Institut für Nuklearforschung SIN, Zürich, Switzerland.

† Present address: Physics Research Laboratory, Massachusetts General Hospital, Boston, Mass.

¹ See, e.g., P. V. Vavilov, Zh. Eksperim. i Teor. Fiz. **32**, 920 (1957) [English transl.: Soviet Phys.—JETP **5**, 749 (1957)]; H. D. Maccabee, M. R. Raju, and C. A. Tobias, Phys. Rev. **165**, 469 (1968); J. J. Kolata, T. M. Amos, and H. Bichsel, *ibid.* **176**, 48 (1968).

² N. Bohr, Phil. Mag. **30**, 581 (1915).

³ K. R. Symon, Ph.D. thesis, Harvard University, 1948 (unpublished).

⁴ C. Tschalär, Nucl. Instr. Methods **61**, 141 (1968).

⁵ C. Tschalär, Nucl. Instr. Methods **64**, 237 (1968).

⁶ M. G. Payne, Bull. Am. Phys. Soc. **13**, 1711 (1968).

⁷ H. W. Lewis, Phys. Rev. **85**, 20 (1952).

Therefore the potential I is, for this simplified spectrum, usually adjusted to give the best agreement of $\kappa_1 = (k/T) \ln(\epsilon T/I)$ with the experimental values $-\langle dT/dx \rangle$.

In the following short review of the pertinent straggling theories, we consider first the earliest one, by Bohr.² The Central Limit Theorem of Statistics states that the sum of a large number of independent stochastic variables tends to be normally distributed, even for arbitrary distributions of the individual variables. The variances of the latter add up to the variance of the sum distribution. This leads to Bohr's expression for σ_2

$$d\sigma_2/dx = \kappa_2, \quad (3)$$

where κ_2 is the variance of $P(Q, T)$. In other words, if the number of random collisions in every collision-energy interval is large, the total energy-loss distribution is expected to be Gaussian, with its variance given by

$$\sigma_2 = 4\pi e^4 z^2 Z N x$$

if Eq. (1) is used. This theory breaks down at larger thicknesses however, since $P(Q, T)$ depends on the residual particle energy T and thus on the energy losses in previous collisions, i.e., individual collisions are not truly independent as required by the Central Limit Theorem.

An improvement was proposed by Symon,³ who derived a series expansion for $d\sigma_n/dx$ and solved for σ_2 , using only the first two terms

$$d\sigma_2/dx = \kappa_2 + 2\sigma_2(d\kappa_1/dT_{av}). \quad (4)$$

The second term describes the broadening of $f(T, x)$ due to the variation of κ_1 over the width of f . Speaking qualitatively, the lower-energy particles in the distribution lose, on average, more energy in each succeeding collision than the higher-energy particles. This effect becomes dominant for large energy losses.

Symon also solved the analogous equation for σ_3 . Due to cancellations, however, the first term that he dropped from the expansion is the dominant contribution to the "skewness" γ_3 .⁴ Therefore, Symon's distributions erroneously remain practically Gaussian up to very large energy losses.

Recently the equations for σ_n were solved numerically⁴ using the single-collision spectrum (1). The results show that the skewness γ_3 increases markedly for large energy losses (e.g., over 80% of T_0 for protons) in contrast to Symon's prediction. However, the values for σ_2 are very close indeed to those of Symon for the region of validity of both theories. For the same region, it was also shown⁴ that κ_1 is very nearly equal to dT_{av}/dx . This allows us to write the equation for the variance σ_2 as

$$d\sigma_2/dx \approx \kappa_1 d\sigma_2/dT_{av} = \kappa_2 + 2\sigma_2(d\kappa_1/dT_{av}).$$

This equation has the analytic solution

$$\sigma_2(T_{av}) = \kappa_1^2(T_{av}) \int_{T_0}^{T_{av}} \frac{dT}{\kappa_1^3} \quad (5)$$

and is valid for an arbitrary collision spectrum, if a correct value of κ_1 is used.

It has been known for some time⁸ that the simple single-collision spectrum (1) should be modified near the low-energy cutoff Q_{min} to include effects due to atomic binding of the interacting electrons. Livingston and Bethe⁸ and Blunck and Leisegang⁹ have studied the increase in κ_2 due to these binding effects. Using Ref. 8, Sternheimer¹⁰ gives some numerical values for the increases. More recently, Shulek¹¹ *et al.* and Golovin¹² *et al.* used a relativistic form of Livingston's expression for κ_2 in order to compute the broadening of the Vavilov distributions¹³ for small energy losses. Unfortunately their values for κ_2 are not available. However, by comparing the widths of Golovin's distributions with those of Vavilov in the limit of large κ , where both are practically Gaussian, the increase in κ_2 due to binding effects can be extracted. With Eq. (5) a correction factor K to the variance of distributions at large energy losses may be calculated numerically. The distributions of Ref. 4 may then be corrected accordingly by multiplying their variances by K , assuming that binding corrections to the skewness are negligible.

The theories discussed so far begin by generating the moments of $f(T, x)$, to which mathematical distributions are then fitted. This procedure has been shown⁵ to break down as soon as the "tail" of f extends to $T=0$ and particles are lost by complete stopping. The failure of the procedure results from the very critical dependence of the skewness parameter γ_3 on the low-energy tail. When this tail is cutoff at $T=0$ with a loss of as few as 0.001% of the particles, the computed value of γ_3 is already about 10% too high. In order to overcome this difficulty, it has been proposed⁵ to propagate numerically the distribution $f(T, x)$, rather than its moments, along x from the point where the previous theory breaks down. In this region statistical effects are largely masked by bulk distortions of $f(T, x)$ through the T dependence of κ_1 , and thus computing times can be reduced to acceptable levels by using a simplified form of $P(Q, T)$.

Most recently Payne⁶ has proposed a new approach. He computes the distributions $h(R, x)$ of residual ranges

⁸ M. S. Livingston and H. A. Bethe, *Rev. Mod. Phys.* **9**, 261 (1937).

⁹ O. Blunck and S. Leisegang, *Z. Physik* **128**, 500 (1950).

¹⁰ R. M. Sternheimer, *Phys. Rev.* **117**, 485 (1960).

¹¹ P. Shulek, B. M. Golovin, L. A. Kulyukina, S. V. Medved, and P. Pavlovich, *Soviet J. Nucl. Phys.* **4**, 400 (1967).

¹² B. M. Golovin, L. A. Kulyukina, S. V. Medved, P. Pavlovich, and P. Shulek, Joint Institute for Nuclear Research, Dubna, Report No. P1-3190, 1967 (unpublished).

¹³ S. M. Seltzer and M. J. Berger, *Natl. Acad. Sci.-Natl. Res. Council, Publ.* **1133**, 187 (1964).

R defined by

$$R(T) \equiv \int_0^T \frac{dT}{\kappa_1}. \quad (6)$$

The functions $h(R,x)$ approach the near-Gaussian shape of the actual range distributions at large energy losses in contrast to $f(T,x)$. They may be obtained by relatively simple fits to their moments. The energy distribution is then given by

$$f(T,x)dT = h(R,x)dR = h(R,x)dT/\kappa_1.$$

The results agree with those of Tschalär's theory^{4,5} to within $\pm 1\%$ of the peak values of $f(T,x)$ for the cases considered below.

The problem of range straggling is intimately related to that of energy straggling, and has been treated theoretically by Lewis⁷ and others, but we do not deal with it here.

III. EXPERIMENTAL METHOD

A. Basic Design

The basic experimental method was to let nearly monoenergetic beams of heavy charged particles impinge normally on plane absorbers of several thicknesses. The energies of the emerging particles were measured by stopping the particles in lithium-drifted silicon-semiconductor detectors, amplifying the output charge pulses due to ionization in the detector, and measuring the magnitude of the pulse from each particle with a multichannel pulse-height analyzer (PHA). Calibration of PHA channel numbers in terms of particle energy is done with standard radioactive sources and a linear test pulse generator by the usual method. There are slight differences in detector response to protons, α particles, and electrons, due to variations of the average energy required to produce an electron-hole pair in the detector. These differences are small enough¹⁴ to be included in the estimated uncertainty of the energy calibration. The print-out information in the form of counts per channel versus channel number may thus be processed to yield a plot of relative frequency versus particle energy, i.e., the energy-straggling distribution. The block diagram of the basic scheme and associated electronics is shown in Fig. 1.

B. 49.10-MeV Protons

The primary beam of the Proton Linear Accelerator at the Rutherford Laboratory was focused onto an aluminum target of thickness 0.025 mm. Protons scattered at 20° were momentum analyzed in a double-focusing magnetic spectrometer. Any extended low-energy tail in the energy distribution of the incident beam was thus eliminated. Such tails arise very easily

¹⁴ R. H. Pehl, F. S. Goulding, D. A. Landis, and M. Lenzlinger, Nucl. Instr. Methods **59**, 45 (1968).

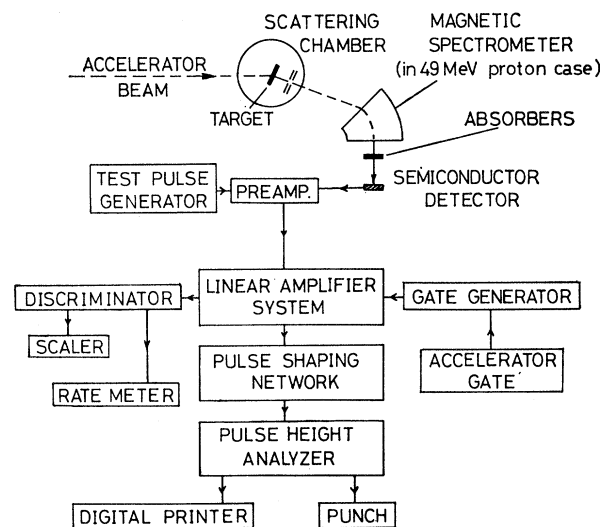


Fig. 1. Schematic diagram of the experimental systems and associated electronics. (Spectrometer used for 49-MeV protons only.)

from slit-edge scattering in the beam transport system. Even if they are of small amplitude they could cause "false" low-energy tails in the measured energy straggling distributions.

At the image plane of the spectrometer, an acoustic spark chamber was mounted in order to measure the radial width of the deflected beam. By using a target in the shape of a strip 0.5 mm high which presented a sharp object line to the spectrometer, the energy spread of the scattered beam was measured to be 50-keV FWHM. With a disk-shaped target the beam was observed to be 2.5 mm wide.

After replacing the spark chamber with a semiconductor detector, a "pin-hole" collimator was scanned across the detector and its sensitive diameter determined to be 8 mm. Subsequently a collimator of 6-mm diameter placed over the detector prevented protons from entering the insensitive region. The depletion depth of the detector was 2 mm.

The detector system was then calibrated with a ThC α -particle source (6.05 and 8.78 MeV). Pulses from a stable ($\pm 0.1\%$) and linear ($\pm 0.1\%$) test-pulse generator were fed to the preamplifier input to provide a reference scale in the recorded pulse-height spectra.

Finally, eight different aluminum and two gold absorbers were consecutively inserted 4 cm in front of the detector and the resulting energy distributions were recorded on the PHA. Since the detector noise equivalent to about 50-keV FWHM was not a limiting factor, the signal pulses were doubly clipped by 1- μ sec delay lines in order to avoid problems of base-line shift and pulse pileup. In this way, average counting rates of about 400 protons per sec could be handled corresponding to an instantaneous rate of 4×10^4 /sec at 1% duty cycle. About 5×10^5 counts were accumulated for each straggling spectrum.

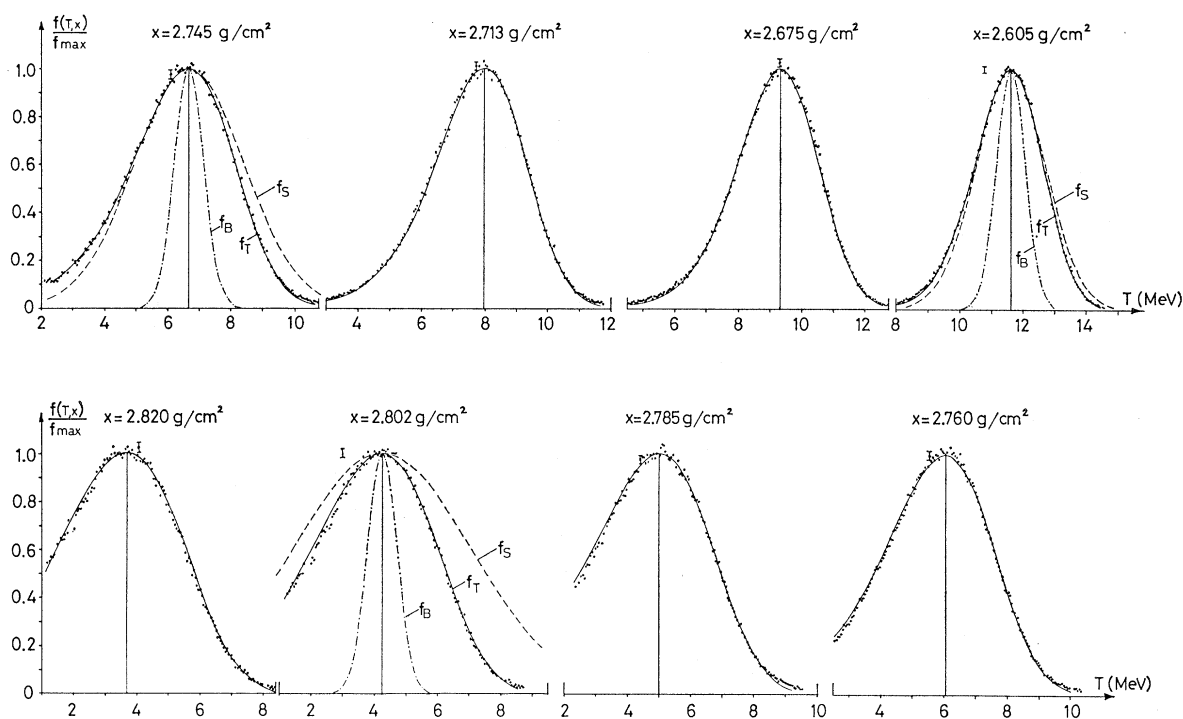


FIG. 2. Energy distributions of 49.10-MeV protons after traversing an aluminum absorber. Curves f_B are theoretical predictions of Bohr (Ref. 2), f_S of Symon (Ref. 3), and f_T of Payne (Ref. 6) and Tschalär (Refs. 4 and 5).

The absorbers were machined from rolled stock to thicknesses uniform within ± 5 mg/cm² (Au) and ± 1 mg/cm² (Al). The surface roughness was less than ± 0.1 mg/cm². In addition, the aluminum absorbers were tested ultrasonically for inhomogeneities.

C. 19.68-MeV Protons and 79.8-MeV Helium Ions

The 88-in. isochronous (sector-focused) cyclotron of the Lawrence Radiation Laboratory, Berkeley was used to produce the incident beams, which were then scattered at a lab angle of 14.1° from a gold target of 200 μ g/cm², and collimated through a 2×5 -mm tantalum aperture. Slit-scattering effects were small, so that no spectrometer energy selection of the initial beam was necessary, but measurements were taken of the initial proton-beam-energy distribution.

The detector had a depletion depth of 3 mm and a noise contribution of less than 25-keV FWHM. The main experimental difficulty was the use of 0.2- μ sec clipping time in the case of one of the absorbers, resulting in inadequate charge collection, and causing a shift in the absolute energy scale which was corrected for in the anomalous case by using range-energy tables to place the peak of the distribution. A Bi-207 electron source (0.48-, 0.98-, and 1.05-MeV) was used in addition to the ThC source for calibration. Six different sets of aluminum absorbers, whose total thicknesses were known to ± 0.5 mg/cm² and whose surface roughnesses were less than ± 0.1 mg/cm², were used consecutively, placed 1 cm in front of the detector. Energy calibration and system resolution were rechecked at the end of the runs. At least 10^5 counts were accumulated per spec-

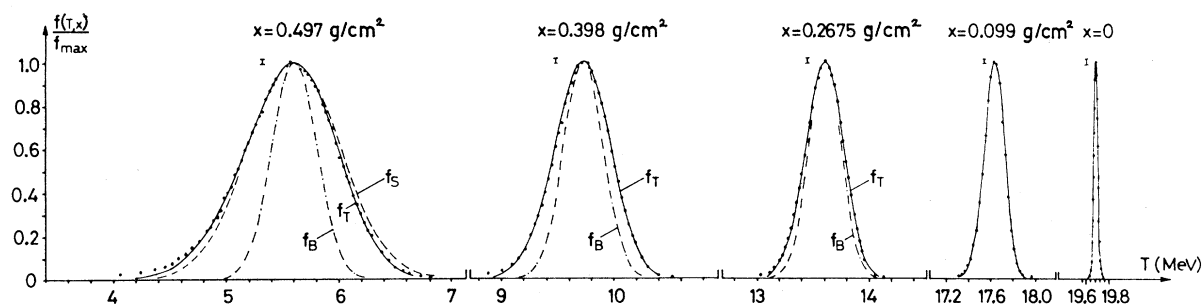


FIG. 3. Energy distributions of 19.68-MeV protons after traversing an aluminum absorber. Curves f_B are theoretical predictions of Bohr, f_S of Symon, and f_T of Payne and Tschalär.

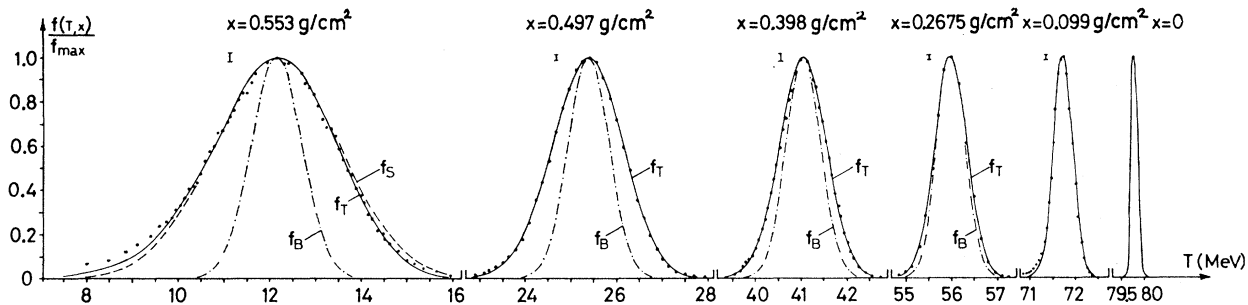


FIG. 4. Energy distributions of 79.8-MeV helium ions after traversing an aluminum absorber. Curves f_B are theoretical predictions of Bohr, f_S of Symon, and f_T of Payne and Tschalär.

trum. Other experimental details were similar to the previous description.

IV. RESULTS

The experimental distributions were normalized to unit peak height rather than unit area, because the area depends somewhat on the experimentally less reliable tails of the distributions. These tails contain, e.g., particles which have lost energy in a nuclear collision or have been scattered into the insensitive region of the detector. As an example, we considered the recorded spectrum of 49.1-MeV protons having traversed 2.675 g/cm² of aluminum (cf. Fig. 2). In this case, 1.8% of the events were contained in the two tail regions extending over 3 MeV from those energies at which the distribution has fallen to 2% of its peak height. The contribution of these regions to the variance σ_2 of the distribution was 15.6%.

The data are shown in Figs. 2-5. The indicated error bars are purely statistical and are calculated as the

square root of the number of counts in each channel. Since the peak height of the distribution was taken as the average over a few channels near the peak, the relative error of the normalization is smaller than the relative statistical error of the peak channels. The relative accuracy of the energy scale was estimated from several test-pulse spectra which were accumulated in regular intervals. The test-pulse pattern was linear, stable, and consistent with the known energies of the simultaneously recorded α and β spectra to within $\pm 0.5\%$ channels over the entire measuring period. The absolute energy calibration was estimated to be accurate within $\pm 0.5\%$, including effects of source thickness, window thickness of the detectors, and differences in the detector response to different particles. The resolution of the system was measured as 30 keV (FWHM of the Bi-207 lines) in the 20-MeV proton case and not more than 50-keV FWHM in the other cases. The resolution correction to the measured spectra was therefore negligible for every absorber case.

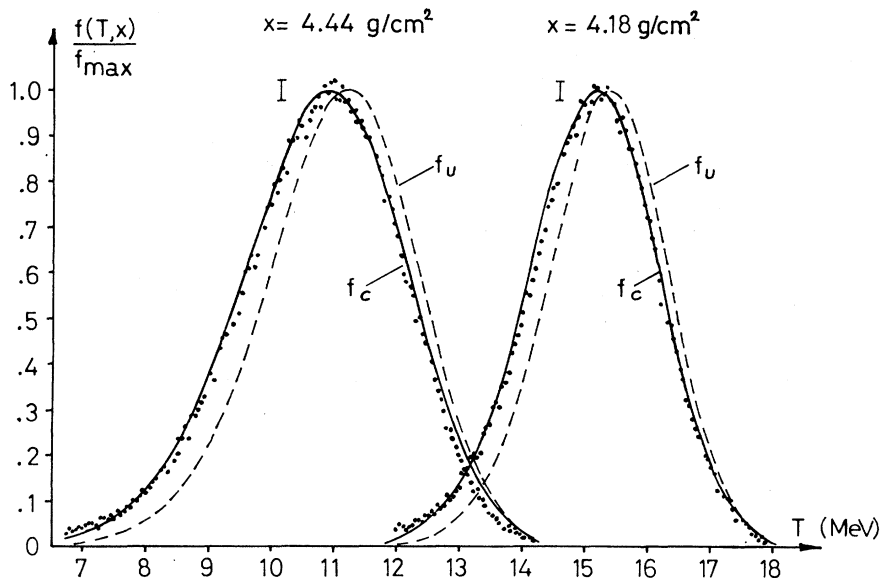


FIG. 5. Energy distributions of 49.10-MeV protons after traversing a gold absorber. Dashed curves f_U are uncorrected theoretical predictions of Tschalär (Refs. 4 and 5). Solid curves f_C are theoretical distributions corrected for resonance broadening and multiple scattering.

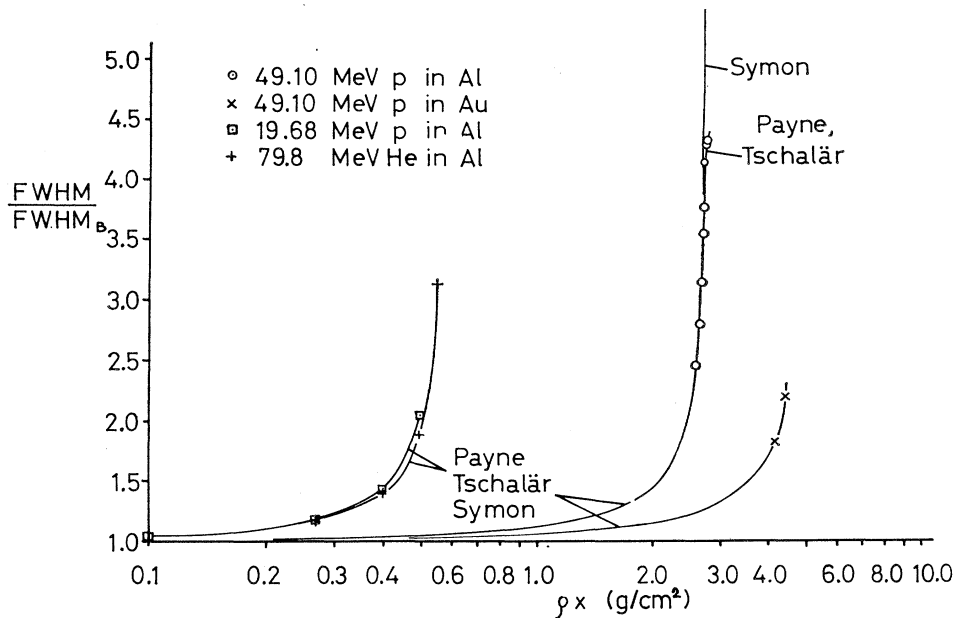


Fig. 6. Ratios of the theoretical distribution widths (Refs. 4 and 5) (FWHM) to the width from Bohr's theory (Ref. 2), as a function of absorber mass thickness. Plotted points are experimental values.

For the aluminum absorbers in Figs. 2–4, the theoretical predictions of Tschalär^{4,5} are shown as solid lines (f_T), those of Symon³ are shown as dashed lines (f_S), and those of Bohr² as dashed-dotted lines (f_B). In all cases the predictions of Payne⁶ deviate from those of Tschalär by less than 1% of the peak value and are not shown separately. For simplicity the curves f_S are drawn as Gaussians, disregarding the slight skewness of the actual Symon distributions.

All theoretical calculations were based on the free-electron single-collision spectrum $P(Q, T)$ of Eq. (1). However, broadening of the distributions by atomic binding effects was calculated from Golovin's tables¹² as described in Sec. II and is included in the theoretical predictions f_T and f_S . These corrections in width amount to about 2% for 49.1-MeV protons in Al, 3% for 19.68-MeV protons and 79.8-MeV α particles in Al, and 9% for 49.1-MeV protons in Au. Furthermore, small relativistic effects were included by replacing the energy T with an energy T' defined as

$$T' \equiv T(1 + T/2Mc^2)/(1 + T/Mc^2) \quad (7)$$

as proposed in Ref. 15 (M = incident particle mass).

The ratios of the theoretical and experimental distribution widths (FWHM) to the width from Bohr's theory are plotted in Fig. 6 as functions of the mass thickness ρx . The accuracy of the experimental widths was estimated from the energy and amplitude uncertainties of the distributions. In all cases, uncertainties of 1 to 2% were found for the FWHM considering that the

widths were measured between two lines drawn through several data points near the half-heights of the distributions.

The I values used were 175 eV for Al, and 930 eV for Au; these values were found to provide classical range functions R_e as defined in Eqs. (1), (2), and (6) which best reproduced our mean energies $\langle T \rangle$ determined from the measured distributions according to Ref. 5. They are larger than the true mean excitation potentials because they have to compensate for the omission of shell corrections from the theory. Figure 7 shows $R_e \langle T \rangle$ for $I_{Al} = 175$ eV and $I_{Au} = 930$ eV, as well as two previously calculated^{16,17} pathlength functions.

Since multiple scattering will increase individual pathlengths, especially in gold absorbers, the experimental mean energies were corrected for the mean increase in pathlength according to Ref. 18. In Fig. 5 the dashed curves f_U represent the theoretical distributions taken from Refs. 4 and 5, uncorrected for multiple scattering and widening by atomic binding. Both these corrections are included in the solid curves f_C . In the case of 20-MeV protons the incident beam energy spread of 40-keV FWHM was taken into account by folding a Gaussian of width $40 \text{ keV} \times [\kappa_1(T_{av})/\kappa_1(T_0)]$ FWHM into the theoretical straggling distributions. The same was done for the 160-keV FWHM spread of the 80-MeV helium ion beam. Corresponding corrections for the 49-MeV proton data were negligible.

¹⁶ C. Tschalär, Ph.D. thesis, University of Southern California, 1967 (unpublished).

¹⁷ J. F. Janni, Air Force Weapons Laboratory Report No. AFWL-65-150, 1966 (unpublished).

¹⁸ C. Tschalär and H. Bichsel, Nucl. Instr. Methods 62, 208 (1968).

¹⁵ C. Tschalär, Rutherford Laboratory Report No. RHEL/R 146, 1967 (unpublished).

V. CONCLUSIONS

Figures 2-6 show that Bohr's theory² does not apply for energy losses greater than about 20% of the initial energy. The deviation from the data is quite dramatic at large energy losses. Symon's theory³ seems to apply down to the region where the straggling distributions become skew. Apart from the skewness, Symon's distributions appear to be too wide for very large energy losses. The predictions of Payne⁶ and Tschalär^{4,5} appear to fit all the aluminum data very well. Widening by atomic binding is quite small in these cases ($\lesssim 3\%$). In particular, the predicted increase in skewness (i.e., low-energy tail) for proton energy losses above 80% of T_0 is confirmed by the experimental data. Small low-energy deviations in the thickest absorber cases for 19.68-MeV protons and 79.8-MeV helium ions are unexplained, but believed to be due to experimental effects.

The fact that experimental distributions in gold are somewhat wider than predicted by Refs. 4-6 is reasonably well explained by atomic binding of the absorber electrons. Still, the corrected distributions f_c appear to be about 2% too wide, which is not surprising in view of the discrepancies between the numerical values of binding corrections from different theories (e.g., Refs. 9-11). Additional widening due to the spreading of pathlengths by multiple scattering could not be detected.

The general agreement indicates that the energy loss of heavy particles in collisions with atomic electrons is sufficiently well described by the free-electron collision-spectrum $P(Q, T')$ of Eqs. (1) and (7) with an atomic-binding correction to its variance, provided that the particle energies are in the region of $0.005 \leq T/Mc^2 \leq 0.05$ and mean energy losses are larger than 10%. The only quantity sensitive to further refinements such as shell corrections, is the mean energy T_{av} of the distributions.

We conclude that the Tschalär^{4,5} and Payne⁶ theories, corrected for atomic binding, are valid in the cases we have studied.

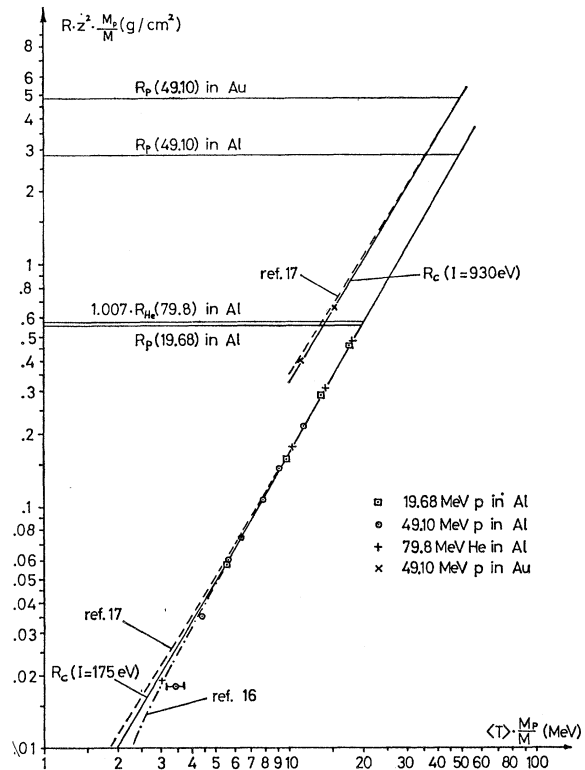


FIG. 7. Classical range functions $R_c\langle T \rangle$, for $I_{Al} = 175$ eV and $I_{Au} = 930$ eV, and proton pathlengths in Al from Refs. 16 and 17 in comparison with experimental data. Experimental energies $\langle T \rangle$ have been corrected for multiple scattering effects.

ACKNOWLEDGMENTS

We express our thanks to the staffs of the Rutherford Laboratory Proton Linear Accelerator and the Lawrence Radiation Laboratory 88-in. cyclotron. We are particularly grateful to F. J. Swales for setting up the P.L.A. high-resolution beam system and to Bob McGrath and Gordon Wozniak for their help with the cyclotron runs.